Constant Flux Illumination of Square Cells for Millimeter-Wave Wireless Communications

Carlos A. Fernandes, *Member, IEEE*, and Luis M. Anunciada

***Abstract*—The use of highly shaped-beam base-station antennas in millimeter-wave wireless communication systems may contribute to significantly enhance system performance. Previously proposed axial symmetric dielectric lenses provide a most useful constant-flux circular footprint, but they may fail to cover the regions near the vertices of square or rectangular cells, unless excessive wall illumination is allowed. This paper presents a simplified procedure to design shaped three-dimensional dielectric lenses that produce constant-flux illumination with square or rectangular footprints, suitable for indoor cells. The procedure is based on circular symmetric dielectric-lens design formulation, yet very sharp rectangular-cell boundary is obtained. Calculated and measured antenna performance is presented, not only in terms of radiation pattern, but also in terms of coverage and time-dispersion characteristic. The procedure is demonstrated for a square-cell lens and is extended for the rectangular-cell case.**

***Index Terms*—Dielectric lenses, millimeter-waves, shaped-beam antennas, wireless communications.**

I. Introduction

THE growing demand for high data rates in the fixed network, driven in part by multimedia applications and computer communication, is gradually extending to wireless systems. The envisaged bandwidths and spectrum congestion at lower frequency bands make millimeter waves attractive for these wireless applications. The mobile broad-band system (MBS) is one example of such systems that was proposed, extensively studied, and demonstrated in the 1990's [1], [2]. Especially at these frequencies, antenna characteristics must be carefully chosen so that the antenna can cooperate with other system components to mitigate the harsh propagation channel impairments.

Previous work has shown that fixed-shaped beam antennas can provide an acceptable compromise between performance enhancement and antenna complexity and cost, enabling data rates up to 170 Msymbol/s without significant mobility restriction [3], [4]. Circular symmetric dielectric lenses were designed to produce $\sec^2\theta$ radiation pattern within a circular cell with quite a sharp boundary. An interesting characteristic of these antennas is that cell radius is proportional to antenna installation height, maintaining constant flux illumination. This provides a simple means to control the amount of energy that illuminates the walls at the cell edge, allowing to choose an adequate compromise between multipath effects and the need for alternative paths in case of line-of-sight (LOS) blocking.

Further improvement of the previous concept can be obtained by adapting the sharp cell boundary produced by the centrally located base-station (BS) lens to the usual rectangular room shape. The limited power available from solid-state devices at millimeter waves is directed only to where it is needed and multipath effects caused by wall illumination are reduced. Circular symmetric lenses fail to cover the regions near the farther walls of the rectangular room, unless excessive illumination of the closer walls is allowed.

A three-dimensional (3-D) lens is required to obtain such coverage. The general formulation for arbitrary 3-D lens design is described in [5], but a less involved approximate procedure is proposed and verified in this paper: the 3-D lens is generated from profiles that are independently calculated for two or three principal planes of the lens. These profiles are obtained from simple formulation developed for circular symmetric lenses, based on geometrical optics (GO). The adopted single-surface dielectric-lens approach is simpler and much more compact then dual-reflector solutions [6] and does not suffer from frontal blocking by the feed. Circular polarization, which is useful to reduce multipath effects, can be easily integrated into this lens configuration and is considered here. This paper addresses not only lens design, but also its assessment in a real scenario providing measured coverage plots and statistical data on received power and signal time dispersion characteristics. The proposed procedure is first demonstrated for square cells and then extended for rectangular cells.

Other antenna approaches reported in the literature for $\sec^2\theta$ coverage in wireless systems at millimeter waves do not pay attention to cell edge geometry [7]–[9] and its implication on system performance.

II. Square-Cell Case

Consider the geometry shown in Fig. 1. The fixed-terminal antenna is mounted near the ceiling at the center of the room and is required to produce $\sec^2\theta$ illumination within a square region that extends from nadir ($\theta = 0$) up to (but excluding) the walls ($0 < \theta < \theta_{\max}$). The desired $\sec^2\theta$ characteristic compensates free-space attenuation at each θ-direction, producing constant flux illumination at constant height everywhere within the cell limits.

Manuscript received March 1, 2001. This work was supported in part by the Fundação para a Ciência e a Tecnologia under Project FCT 34860/99.

C. A. Fernandes is with the Instituto Superior Técnico, Instituto de Telecomunicações, 1049-001 Lisbon, Portugal (e-mail: carlos.fernandes@lx.it.pt).

L. M. Anunciada was with the Instituto Superior Técnico, Instituto de Telecomunicações, 1049-001 Lisbon, Portugal. He is now with Ericsson Telecomunicações Lda., 2780-730 Paço de Arcos, Portugal (e-mail: luis.anunciada@sep.ericsson.se).

Publisher Item Identifier S 0018-9480(01)09383-8.

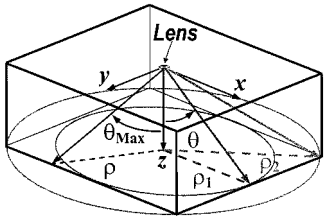

Fig. 1. Cell geometry.

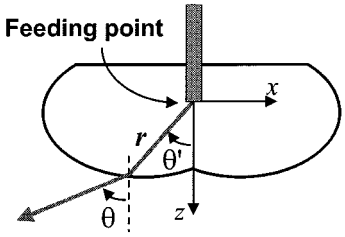

Fig. 2. Basic dielectric-lens configuration.

A. Lens Design

The basic lens configuration is shown in Fig. 2. The lens is fed by the circularly polarized TE_{11} mode of a circular waveguide that is immersed in the lens body. The waveguide is aligned with a lens z-axis and with a cell vertical axis.

An approximate procedure is adopted for the lens design. The 3-D lens surface $r(\theta', \varphi')$ is generated from two profiles that are independently calculated for lens $\varphi' = 0$ and $\varphi' = \pi/4$ planes. The lens is positioned such that the $\varphi' = 0$ plane is perpendicular to one room wall and the $\varphi' = \pi/4$ plane is aligned with the room diagonal. Note that the maximum elevation angle $\theta_{\max}$ that defines the cell edge is a function of the azimuth angle φ, being minimum for $\varphi = \pm n\pi/2$ and maximum for $\varphi = \pi/4 \pm n\pi/2$.

The lens profiles for the $\varphi' = 0$ and $\varphi' = \pi/4$ planes are taken as equal to the profiles of circular symmetric lenses designed to produce circular cells with radius ρ_1 and ρ_2, respectively (half-side and half-diagonal of the room), when located at a common height ΔH above the mobile. The design of circular symmetric lenses is based on GO formulation. The procedure is well established [3], [4] and will not be repeated here. The lens profile obtained for $\varphi' = 0$ will henceforth be referenced with index 1 and the profile for $\varphi' = \pi/4$ with index 2. The 3-D lens surface $r(\theta', \varphi')$ is generated by the combination of profiles 1 and 2 according to the heuristic equation

$$r(\theta', \varphi') = r_1(\theta') + \frac{\Delta r}{2}\left[1 + \sin\left(4\varphi' - \frac{\pi}{2}\right)\right] \quad (1a)$$

$$\Delta r = r_2(\theta') - r_1(\theta') \quad (1b)$$

where $r_1(\theta')$ represents profile 1 and $r_2(\theta')$ represents profile 2. They are calculated subject to the initial condition $r_1(0) = r_2(0)$. From the above expression, $r(\theta', \varphi')$ coincides with profile 1 for $\varphi' = n\pi/2$ and with profile 2 for $\varphi' = \pi/4 + n\pi/2$. This procedure yields good results when Δr does not exceed $\sim$10% of $r_1(\theta')$ at any point of the lens. Otherwise, refraction in the horizontal plane (which does not exist in circular symmetric lenses) may significantly change the elevation pattern with respect to a circular symmetric lens with the same profile.

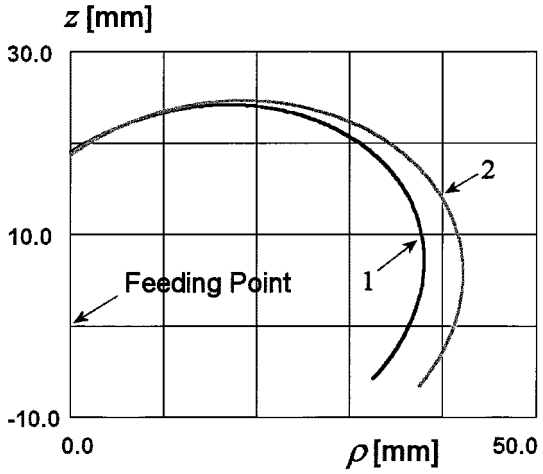

(a)

(b)

Fig. 3. Dielectric-lens antenna for a square cell, fed by a circular waveguide. (a) Lens profiles 1 and 2. (b) Constructed lens.

B. Simulation and Experimental Results

Using the proposed procedure, a dielectric lens is designed to produce $\sec^2\theta$ illumination within a square spot of 10 m $\times$ 10 m when positioned 1.5 m above the mobile terminal antenna level. The lens is designed for 60-GHz-band operation. Fig. 3(a) shows the lens profiles calculated for $\varphi' = 0$ and $\varphi' = \pi/4$ planes. The fabricated Plexiglas prototype ($\varepsilon_r = 2.53$, $\tan\delta = 0.012$) is shown in Fig. 3(b). A reasonably compact lens is obtained (the lens diagonal is 84 mm and the lens depth is 32 mm). This is henceforth referred to as Lens-1. The corresponding elevation power patterns shown in Fig. 4(a) are measured for the $\varphi = 0$ and $\varphi = \pi/4$ planes. They comply well with the desired $\sec^2\theta$ characteristic in both planes and with the required $\theta_{\max}$ specification. Radiation falls off rapidly for $\theta > \theta_{\max}$, meaning that this lens will hardly see ceiling reflection paths. Ripple is due to the lens internal reflections. These can be reduced, but the required procedure is not discussed in this paper.

In order to demonstrate the effectiveness of Lens-1 to produce a square-shaped cell with constant flux illumination, continuous wave (CW) measurements were carried out in a 10.8 m $\times$ 8.7 m laboratory cluttered with normal furniture. A previously designed omnidirectional lens antenna [4], hereafter referred to as Lens-2, was used at the portable terminal and displaced along several straight paths in the room at constant height $h_m = 1.6$ m, while retrieving the received power. Besides being independent of the

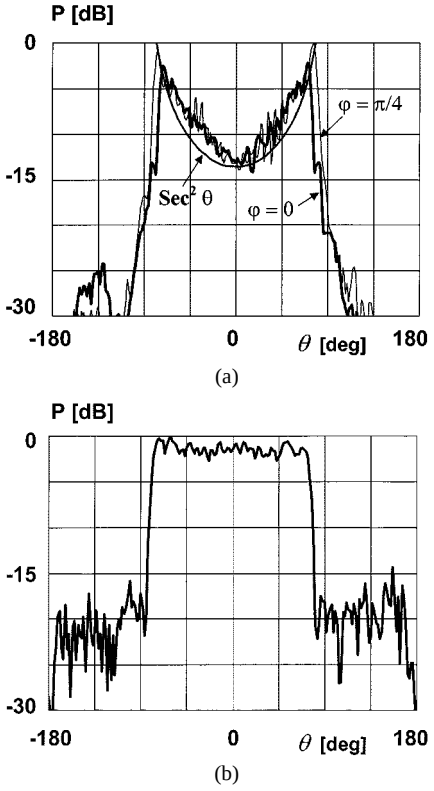

Fig. 4. Power patterns measured at 62.5 GHz. (a) Lens-1, used for fixed terminal ($D = 8.5$ dBi). (b) Lens-2, used for moving terminal ($D = 5.3$ dBi).

azimuth angle φ, the radiation pattern of the moving antenna is also independent of the elevation angle within a compatible elevation interval [see Fig. 4(b)], which eliminates movement restrictions. The sharp fall of radiation for $\theta > 76°$ greatly reduces ground reflection pickup. This antenna also operates in circular polarization. The resulting power distribution over the laboratory is shown in Fig. 5(a) for $\Delta H = 0.5$ m and in Fig. 5(b) for $\Delta H = 1$ m. Measurements were skipped in the white spot near the center, where the lens antenna support structure and equipment blocked the path. The square shape of the illuminated region is quite apparent, as well as the sharp boundary. Fig. 5 also confirms that, intrinsic to the $\sec^2\theta$ illumination, the length of the illuminated square region is proportional to ΔH.

A quantitative measure of coverage and time dispersion can be obtained from Fig. 6, which shows the cumulative distribution function (CDF) of normalized received power (NRP) and the CDF of sliding delay window parameter containing 90% of the energy of the channel impulse response (SDW90%). These are simulated results and correspond to different values of ΔH in the empty room.

They confirm that room coverage improves until $\Delta H = 1.5$ m (when the illuminated region reaches the walls). In this limit, SDW90% becomes less then 3 ns for 100% of the room, which enables very high data transmission rates even without an equalizer. Increasing ΔH further does not change much in this case because of the circular polarization used in both antennas.

III. Extension for Rectangular Cells

The previous design procedure can be extended for rectangular cells, provided that cell length to width ratio is not significantly larger that unity. Three lens principal planes need to be defined: plane $\varphi' = 0°$, which is perpendicular to the farther walls of the rectangular room, plane $\varphi' = \varphi_0$, which is aligned with room diagonal, and plane $\varphi' = \pi/2$, which is perpendicular to the closer walls. Three lens profiles, i.e., $r_1(\theta')$, $r_2(\theta')$, and $r_3(\theta')$ associated with the above planes, are calculated from circular symmetric lenses as described for the square lens in Section II-A. The heuristic expression (2) is used for generation of the 3-D lens surface $r(\theta', \varphi')$, from the above $r_1(\theta')$, $r_2(\theta')$, and $r_3(\theta')$ profiles

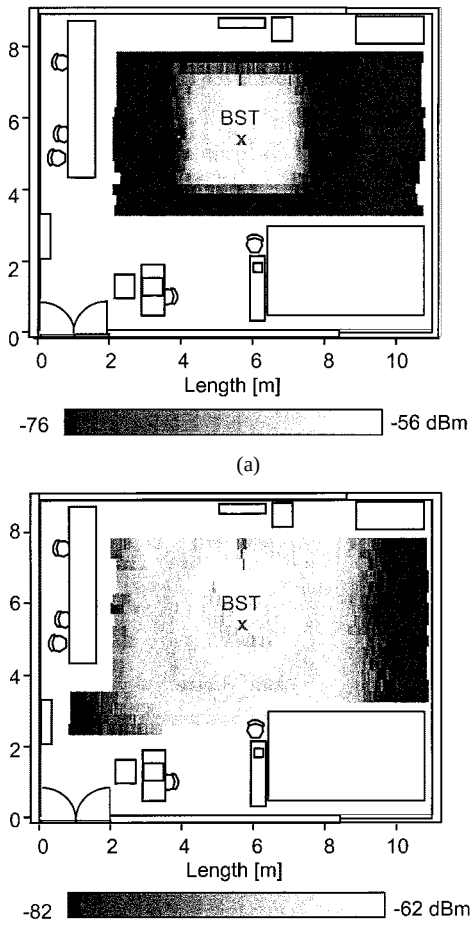

Fig. 5. Received power distribution measured in the laboratory at 62.5 GHz, for the combination of Lens-1 and Lens-2. (a) $\Delta H = 0.5$ m, $h_b = 2.0$ m. (b) $\Delta H = 1$ m, $h_b = 2.5$ m.

$$r(\theta', \varphi') = r_a(\theta', \varphi') + \frac{\Delta r}{2}\left[1 + \sin\left(4\varphi_a - \frac{\pi}{2}\right)\right] \quad (2)$$

where

$$\Delta r = r_2(\theta') - r_a(\theta', \varphi') \quad (3a)$$

$$r_a(\theta', \varphi') = r_3(\theta') + \frac{\Delta r_a}{2}\left[1 + \sin\left(2\varphi' + \frac{\pi}{2}\right)\right] \quad (3b)$$

$$\Delta r_a = r_1(\theta') - r_3(\theta') \quad (3c)$$

$$\varphi_a = \varphi' + a\sin(2\varphi') \quad (3d)$$

$$a = \frac{\frac{\pi}{4} - \varphi_0}{\sin 2\varphi_0}, \qquad \frac{\pi}{4} - \frac{\pi}{10} < \varphi_0 < \frac{\pi}{4} + \frac{\pi}{10}. \quad (3e)$$

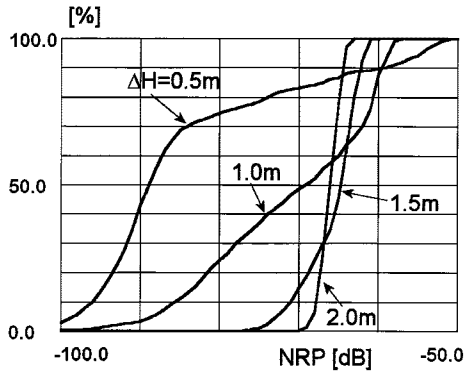

(a)

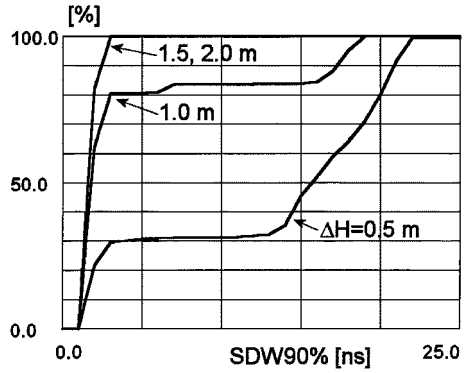

(b)

Fig. 6. CDF of NRP and SDW90% for different values of ΔH.

The resulting surface $r(\theta', \varphi')$ has continuous derivatives with respect to θ' and φ' and coincides with $r(\theta')$ for $\varphi' = 0$ and π, with $r_2(\theta')$ for $\varphi' = \varphi_0$ and with $r_3(\theta')$ for $\varphi' = 0$ and $3\pi/2$. Expression (1) presented in Section II-A for the square-cell lens is a particular case of the above expressions, when $r_1(\theta') = r_3(\theta')$ and $\varphi_0 = \pi/4$. Note that the room diagonal angle φ_0 in (3e) is restricted to a narrow interval to ensure small values of $\partial r/\partial \varphi'$. A different lens design approach exists for extremely elongated rectangular cells [10].

Fig. 7 shows the principal plane profiles of a dielectric lens designed according to the above procedure to produce constant flux illumination within a rectangular area with 12 m×8 m, when located 1.5 m above the mobile antenna level. Thus, $\theta_{\max}$ is taken as 76°, 78°, and 69.5° for the design of profiles 1–3, respectively. As in the previous case, the lens is fed by the TE_{11} mode of the circular waveguide, with circular polarization. It will be referenced as Lens-3.

The simulated distribution of the NRP shown in Fig. 8 corresponds to Lens-3, when centrally positioned in a 8 m × 12 m × 6 m (width (W), length (L), and height (H), respectively) room, at 1 m above the mobile terminal antenna level. The measured circularly polarized radiation pattern of Fig. 4(b) is used for the mobile antenna in these simulations. The obtained cell boundary is reasonably rectangular and sharp, and, as expected, its dimensions are shown to change linearly with the antenna height difference ΔH. Simulation results for the NRP and SDW90% in this case are very similar to those presented in Fig. 6 for the square cell. This proves the effectiveness of the shaped radiation patterns of BS and mobile antennas and the benefit obtained from circular polarization.

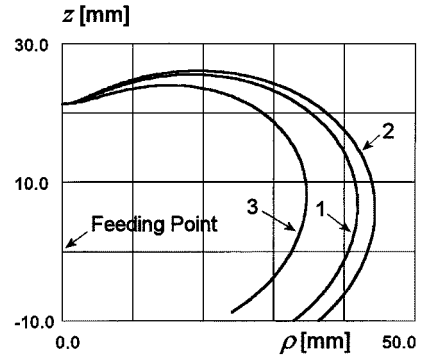

Fig. 7. Principal plane profiles of dielectric lens for rectangular cell (Lens-3).

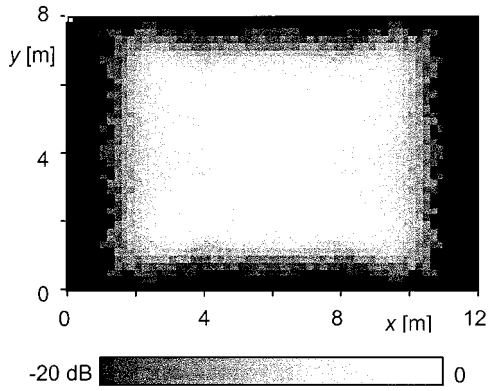

Fig. 8. Received power distribution (normalized to maximum) calculated at 62.5 GHz for the combination of Lens-3 and Lens-2. $\Delta H = 1$ m, $h_b = 2.5$ m.

However, simulations also show that circular polarization can be a disadvantage when the LOS path between the transmitter and receiver is blocked, even when ΔH is larger than the lens design value ($\Delta H = 1.5$ m in this example), a situation where the walls become illuminated. The thick line of Fig. 9 shows the CDF of the NRP obtained in the same room of Fig. 8 for the combination of Lens-3 and Lens-2, but removing the contribution from the LOS path for every position of the mobile antenna in the cell. Only the contributions from reflection paths are retained. This is an extreme and unlikely situation to happen everywhere in the room, but it gives the worst-case design condition. The increase of signal level in the room with ΔH in these conditions is weak for circular polarization.

Linear polarization (thin line) is preferred when LOS blocking probability is high. The linear polarization curves in Fig. 9 correspond to Lens-4, designed with the same specifications of Lens-3, but fed by the circular waveguide TM_{01} mode. However, Lens-4 is paired with the previous Lens-2 at the mobile terminal, which uses circular polarization. The increase in received power level with ΔH in non-LOS conditions is higher then for the Lens-3 case. As a drawback, it is noted that because on-axis radiation is null for linear polarization, an under-illuminated spot appears near the center of the room.

As a general rule, for circular polarization, the BS lens must be installed as high as possible in the center of the room, with a footprint designed to prevent wall illumination. In this way, the LOS blocking probability is reduced and gain is enhanced. With linear polarization, BS antenna height can be adjusted to control

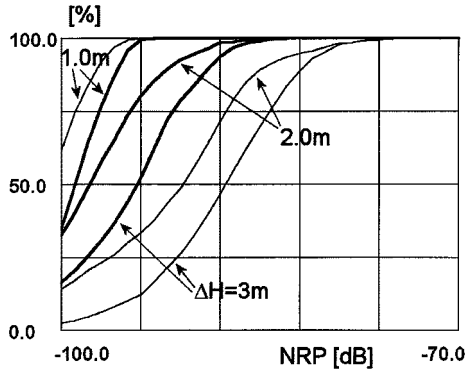

Fig. 9. CDF of the NRP in non-LOS conditions for different values of ΔH. Thick line: circular polarization (Lens-3 and Lens-2), thin line: linear polarization (Lens-4 and Lens-2).

the amount of wall illumination as a compromise between multipath effects and the need for alternative paths in case of LOS blocking.

IV. Conclusions

An easy-to-design compact 3-D-dielectric lens is proposed to produce $\sec^2\theta$ illumination with a square or rectangular footprint, intended for the BS of wireless millimeter-wave communication systems. The design procedure relies on simple formulation for circular symmetric lenses based on GO. It is valid for target rectangular-cell shapes with moderate length to width ratio.

The developed BS lens can be paired with a hemispherical lens antenna at the mobile terminal when high mobility is required, or with other high gain antennas for quasi-static terminals. Besides constant flux, shaping the cell boundary contributes to conservation of power and favors the reduction of multipath effects. Using the correct lens antenna installation height, almost 100% of the room is illuminated with an appropriate signal level and negligible time dispersion, enabling high data transmission rates.

A 84 mm $\times$ 32 mm (diagonal $\times$ depth) lens prototype was fabricated and experimentally assessed in anechoic chamber measurements and coverage measurements in a real scenario at 62.5 GHz, showing good agreement with developed prediction tools. No optimization was tried for the constructed prototype, although it can be easily integrated into the design procedure. A computer numeric control (CNC) milling machine was used to produce the 3-D lens surface, but molding can be used in mass production to obtain very inexpensive antennas.

Acknowledgment

The authors are indebted to P. Lourenço, Instituto Superior Técnico, Lisbon, Portugal, and P. Rocha, Instituto Superior Técnico, Lisbon, Portugal, for assistance with the CNC milling of the lens prototype.

References

[1] L. Fernandes, "Developing a system concept and technologies for mobile broadband communications," *IEEE Pers. Commun.*, vol. 2, pp. 54–59, Feb. 1995.

[2] M. Dinis, J. Fernandes, M. Prögler, and W. Herzig, "The SAMBA trial platform in the field," in *Proc. ACTS Mobile Commun. Summit*, Sorrento, Italy, 1999, pp. 1013–1018.

[3] C. A. Fernandes, V. Brankovic, S. Zimmermman, M. Filipe, and L. Anunciada, "Dielectric lens antenna for wireless broadband communications," *Wireless Pers. Commun. J.*, vol. 10, no. 1, pp. 19–32, June 1999.

[4] C. A. Fernandes and J. G. Fernandes, "Performance of lens antennas in wireless indoor millimeter-wave applications," *IEEE Trans. Microwave Theory Tech.*, vol. 47, pp. 732–737, June 1999.

[5] C. Salema, C. Fernandes, and R. Yha, *Solid Dielectric Horn Antennas*. Norwood, MA: Artech House, 1998.

[6] M. Orefice, "A shaped-omnidirectional pattern dual reflector antenna for millimeter waves," in *Proc. IEEE AP-S Int. Symp. Dig.*, Atlanta, GA, 1998, pp. 844–844.

[7] Y. Murakami *et al.*, "A switchable four-sector shaped-beam antenna for millimeter wave wireless LAN's," in *Proc. IEEE AP-S Int. Symp. Dig.*, Atlanta, GA, 1998, p. 2248.

[8] P. Besso *et al.*, "Design and characteristics of a sector/cosec2 shaped beam microstrip antenna," in *Proc. IEEE AP-S Int. Symp. Dig.*, Eindhoven, The Netherlands, 1995, p. 85.

[9] B. Kolundzija, V. Brankovic, and S. Zimmermann, "Feasibility study of millimeter wave metal antennas," in *Proc. RACE Mobile Telecommun. Summit*, Granada, Spain, 1996, p. 295.

[10] C. A. Fernandes, "Design of shaped lenses for non-Symmetric cells in MBS," in *Proc. IEEE AP-S Int. Symp. Dig.*, Orlando, FL, July, pp. 2440–2443.

Carlos A. Fernandes (S'86–M'89) received the Licenciado, M.Sc., and Ph.D. degrees in electrical and computer engineering from the Instituto Superior Tècnico (IST), Instituto de Telecomunicacções, Portugal, in 1980, 1985, and 1990, respectively.

In 1980, he the Department of Electrical and Computer Engineering, IST, where, since 1993, he has been an Associate Professor. Since 1993, he has also been a Senior Researcher at the Instituto de Telecommunicações, where he has been the Leader of the antenna activity in both national and European projects such as RACE 2067-MBS and ACTS AC230-SAMBA (system for advanced mobile broad-band applications). He co-authored a book, a book chapter, and several technical papers in international journals and conference proceedings in the areas of antennas and radio-wave propagation modeling. His current research interests include dielectric antennas for wireless millimeter-wave applications and propagation modeling for mobile communication systems.

Luis M. Anunciada, photograph and biography not available at time of publication.